

Diterpenoids from the Mediterranean Brown Alga *Dictyota* sp. Evaluated as Antifouling Substances against a Marine Bacterial Biofilm

Yannick Viano, Dominique Bonhomme, Mercedes Camps, Jean-François Briand, Annick Ortalo-Magné, Yves Blache, Louis Piovetti, and Gérald Culioli*

Laboratoire MAPIEM (EA 4323), Université du Sud Toulon-Var, Avenue de l'Université, BP 20132, F-83957 La Garde Cedex, France

Received February 17, 2009

Four new cyclized diterpenes, one xenicane (**1**) and three dolabellanes (**2–4**), were isolated, along with seven previously reported metabolites [3β -hydroxydilophol (**5**), dictyols E (**6**) and C (**7**), hydroxycrenulide (**8**), 9-acetoxy-15-hydroxy-1,6-dollabelladiene (**9**), hydroxyacetyldictyolal (**10**), and fucoxanthin], from a Mediterranean species of *Dictyota* sp. collected in Le Brusc Lagoon (French Mediterranean coast). Their structures, as well as their relative configurations, were determined through extensive spectrometric (IR, HRESIMS, 1D and 2D NMR) data analysis and molecular modeling studies and by comparison with those reported in literature. Some of the isolated metabolites were evaluated for their antiadhesion activity against a marine bacterial biofilm (*Pseudoalteromonas* sp. D41).

All surfaces immersed in the marine environment are subject to colonization by micro- (bacteria and microalgae) and then macro-organisms (macroalgae and invertebrates), which results in the formation of a complex biological layer. This process is called biofouling. Bacteria are of special importance because they are the first colonizers of free surfaces and they are also known to be implicated in the regulation of the subsequent settlement by invertebrate larvae.¹ After an initial step of attachment to a surface, bacteria develop into a complex, organized, three-dimensional community.² These bacterial biofilms, which confer a high degree of protection to the cells, are particularly resistant, and thereby new developments in effective biocides are needed.³

Among brown algae, *Dictyota* species are the most significant producers of secondary metabolites, especially diterpenoids.⁴ These compounds can generally be divided according to their carbon skeleton into three groups: xenicanes, dolabellanes, and “extended sesquiterpenes”. Biological studies have shown a great number of these diterpenoids to possess algicidal,⁵ antibacterial,^{6–10} antifungal,¹¹ antiviral,^{12,13} cytotoxic,^{14–17} antifeedant,^{10,18–20} or antifouling^{21,22} activities.

In continuation of our project centered on the isolation of bioactive metabolites from marine algae,^{23–25} we have initiated a study on the chemical composition of the brown alga *Dictyota* sp. collected from the French Mediterranean coast (Le Brusc Lagoon, Var), which has afforded 11 compounds. These include one novel xenicane (**1**) and three novel dolabellane (**2–4**) diterpenoids together with six known diterpenes (**5–10**) and the carotenoid fucoxanthin. The planar structures of these metabolites were characterized by extensive spectroscopic analysis and by comparison of the data with those of related compounds. Assignments of relative configurations were accomplished by extensive NOE and molecular modeling studies. The bioactivity of metabolites isolated in sufficient amount (**3**, **4**, **6–9**, and fucoxanthin) was evaluated against a marine bacterial biofilm (*Pseudoalteromonas* sp. D41) with the aim of screening new potential natural antifoulants.

Results and Discussion

Shade-dried thalli of *Dictyota* sp. were extracted with a mixture of $\text{CHCl}_3/\text{MeOH}$. The lipophilic fraction of the crude extract was concentrated and fractionated by gravity column chromatography. The eluted fractions were further purified by reversed-phase HPLC to yield four new diterpenes (**1–4**) in addition to seven known

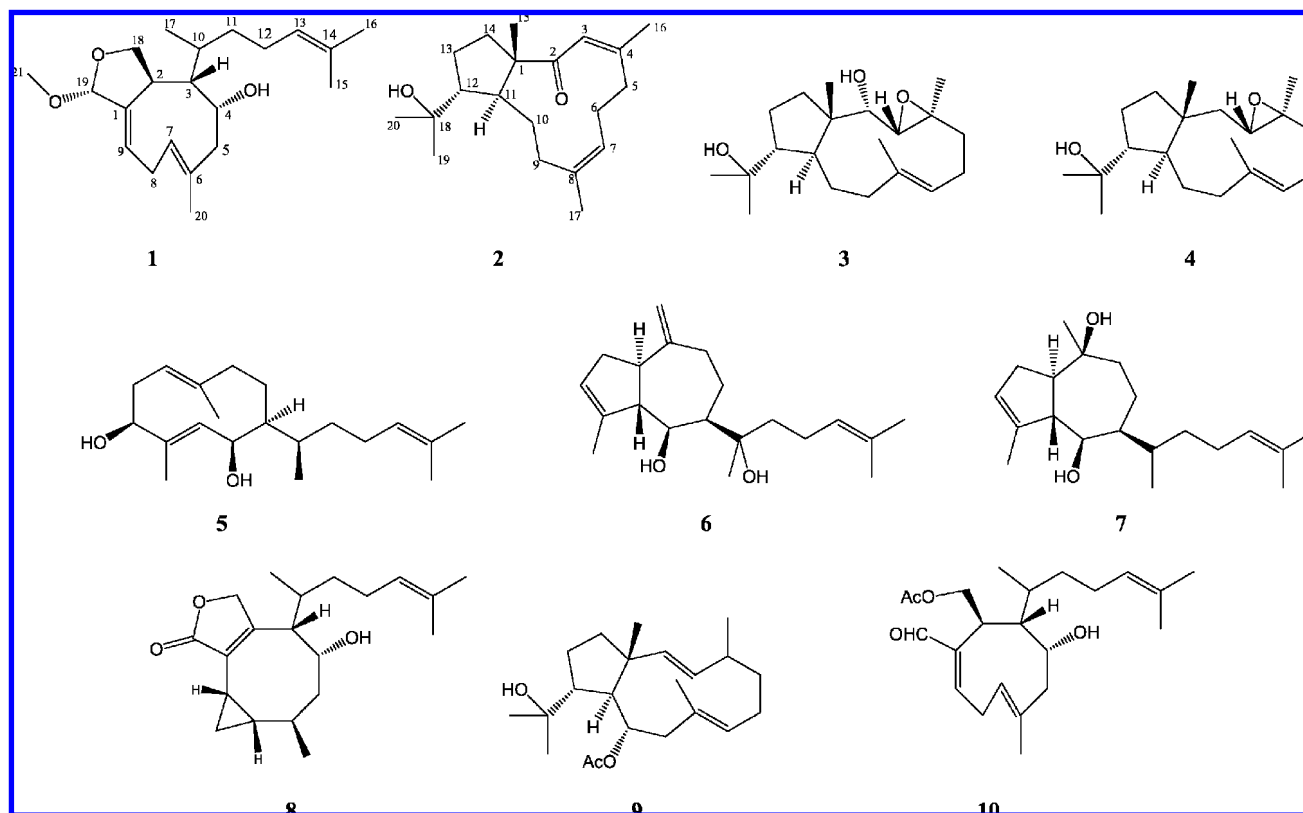
compounds [3β -hydroxydilophol (**5**),²⁶ dictyols E (**6**) and C (**7**),²⁷ hydroxycrenulide (**8**),^{13,28,29} 9-acetoxy-15-hydroxy-1,6-dollabelladiene (**9**),^{14,30,31} hydroxyacetyldictyolal (**10**),³² and fucoxanthin³³].

Compound **1** was obtained as a colorless oil and gave an $[\text{M} + \text{H} - \text{MeOH}]^+$ ion by HRESIMS at m/z 303.2339 for a molecular formula of $\text{C}_{21}\text{H}_{34}\text{O}_3$. ^{13}C NMR analysis revealed the presence of three quaternary, eight methine, five methylene, and five methyl carbons (Table 1). The absence of absorbances in the IR spectrum of **1** for carbonyl and the lack of signals above 150 ppm in its ^{13}C spectrum clearly illustrated that all oxygen functionalities within it are in the form of hydroxy or ether groups. This deduction was supported by (i) IR absorption bands for hydroxy (3472 cm^{-1}) and ether (1112 and 1076 cm^{-1}) functional groups and (ii) ^{13}C NMR resonances at δ_{C} 69.8, 73.1, and 105.7. As six of the downfield carbons (δ_{C} 148.8, 134.8, 131.3, 126.7, 124.9, and 124.6) were assigned as olefinic or aromatic carbons, and considering that the molecular formula indicated the existence of five double-bond equivalents, **1** must be bicyclic. The ^1H NMR spectrum in CDCl_3 (Table 2) showed again five methyl groups [three vinylic methyl singlets (δ_{H} 1.59, 1.68, and 1.86), one methyl doublet (δ_{H} 1.09, $J = 7.0\text{ Hz}$), and one methyl singlet attributed to a methoxy group (δ_{H} 3.40)], five deshielded methine protons (δ_{H} 5.84, 5.34, 5.19, 5.08, and 4.26), and one oxymethylene group [δ_{H} 3.81 (1H) and 4.09 (1H)], as well as signals with complex coupling patterns attributed to methylene and methine protons. After the unequivocal attribution of proton and protonated carbon signals in the ^{13}C NMR spectra of **1** by the HSQC experiment, the results of the HMBC and $^1\text{H}-^1\text{H}$ COSY experiments (Figure 1) allowed the structure to be established as a nine-membered ring substituted by a typical 6-methyl-5-hepten-2-yl side-chain. Thus, the skeleton of **1** could be deduced as that of a xenicane with an extra carbon in the form of a methoxy group. In addition, HMBC correlations between C-4 and H-3 and H-5b, on one hand, and $^1\text{H}-^1\text{H}$ COSY cross-peaks between H-4 and H-5a,b on the other permitted localization of the hydroxy group at C-4 on the cyclononadiene part. Moreover, the presence of an acetal methine group in **1** was indicated by typical NMR signals (δ_{H} 5.19 and δ_{C} 105.7), and specific HMBC correlations suggested that the C-19 carbon atom was part of an acetal ring structure with C-18, also involving the methoxy group. The *E* configuration was assigned to the Δ^6 double bond on the basis of an NOE correlation between H-7/H-5a and H₃-20/H-8b, as well as the upfield shift of the C-20 vinyl methyl carbon at δ_{C} 19.9.

In order to determine the configuration of the Δ^9 double bond and the relative configuration at C-2, C-3, and C-4 of **1**, molecular

* To whom correspondence should be addressed. Tel: (33) 494 142 935. Fax: (33) 494 142 168. E-mail: culioli@univ-tln.fr.

Chart 1

**Table 1.** ^{13}C NMR Data for Compounds 1–4 (100 MHz in CDCl_3)

position	1	2	3	4
	δ_{C} , mult. ^a	δ_{C} , mult.	δ_{C} , mult.	δ_{C} , mult.
1	148.8, qC	57.8, qC	48.4, qC	43.7, qC
2	38.9, CH	208.7, qC	81.7, CH	41.3, CH ₂
3	49.7, CH	121.6, CH	66.3, CH	63.9, CH
4	73.1, CH	154.4, qC	63.9, qC	62.5, qC
5	49.0, CH ₂	32.1, CH ₂	39.9, CH ₂	38.8, CH ₂
6	134.8, qC	21.7, CH ₂	24.3, CH ₂	24.4, CH ₂
7	126.7, CH	124.2, CH	125.6, CH	125.9, CH
8	29.2, CH ₂	135.4, qC	133.6, qC	134.0, qC
9	124.9, CH	28.6, CH ₂	37.8, CH ₂	37.6, CH ₂
10	31.0, CH	28.9, CH ₂	33.7, CH ₂	32.5, CH ₂
11	38.4, CH ₂	45.6, CH	37.2, CH	41.2, CH
12	26.1, CH ₂	55.8, CH	61.3, CH	61.0, CH
13	124.6, CH	27.8, CH ₂	27.0, CH ₂	26.3, CH ₂
14	131.3 qC	39.8, CH ₂	44.3, CH ₂	44.7, CH ₂
15	17.7, CH ₃	16.7, CH ₃	23.2, CH ₃	23.2, CH ₃
16	25.7, CH ₃	30.4, CH ₃	17.6, CH ₃	16.8, CH ₃
17	18.6, CH ₃	22.6, CH ₃	16.5, CH ₃	16.2, CH ₃
18	69.8, CH ₂	73.9, qC	72.4, qC	72.4, qC
19	105.7, CH	26.6, CH ₃	30.1, CH ₃	28.0, CH ₃
20	19.9, CH ₃	29.8, CH ₃	30.1, CH ₃	30.7, CH ₃
21	55.0, CH ₃			

^a Multiplicities inferred from DEPT and HSQC experiments.

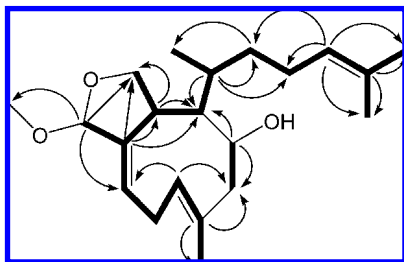
models of all the corresponding diastereoisomers were constructed and subjected to conformational search using the molecular dynamics procedure, and the resulting geometries were optimized by semiempirical calculations (data shown in Table S5, Supporting Information). The NMR data showed (i) an almost 0 Hz coupling constant between H-2/H-3 and H-3/H-4 implying a nearly 90° dihedral angle between protons of each pair, (ii) strong NOE correlations between H-3/H-7 and H-2/H₃-20, and (iii) a *cis* relationship between H-3 and H-4 based on NOE correlations between respectively H-4/H-5a, H-5a/H-7, and H-3/H-7. Thus, this molecular modeling study demonstrated that only one diastereoisomer (2*S**, 3*S**, 4*R**, 9*E*) was in accordance with these selected

experimental data (Table 3). It could be pointed out that the relative configuration obtained for these stereocenters was consistent with those of hydroxyacetyldictyolal (**10**)^{32,34,35} and related xenicanes previously isolated from Dictyotaceae.^{6,36,37} Next, the effect of the configuration of the stereocenter at C-19 in the second ring has been evaluated on these molecular models (Table S6, Supporting Information). In each case, changes of configuration at C-19 did not affect the selected data used to discriminate the different diastereoisomers. Interestingly **1** was found to be unstable in chloroform, leading to a significant change to the chemical shift of H-19 (from δ_{H} 5.19 to δ_{H} 4.93). Further, a new NOE correlation was observed between H-19 and H-9. An explanation of this phenomenon may be the epimerization of **1** at C-19. To this aim, the geometries of the two possible stereoisomers **1a** and **1b** were optimized (Figure 2), and the distances between H-19 and H-9 (2.93 Å for **1a** vs 2.59 Å for **1b**) were calculated from modeling: these data supported the configuration at C-19 for **1** to be as shown in **1a**. In addition, semiempirical calculations showed that **1b** appears to be more stable than **1a** ($\delta\Delta H_{\text{f}}^{\circ} = -11.3$ kJ/mol), explaining a slow displacement of the equilibrium from **1a** to **1b**. Concerning the configuration at C-10, X-ray diffraction analyses carried out on similar xenicanes isolated from Dictyotaceae have determined a 10*R** configuration.^{6,37} In the case of **1**, as it has not been possible to obtain suitable crystals, there was no determination of the configuration at this stereocenter. Therefore, the relative configuration of the whole molecule was proposed to be 2*S**, 3*S**, 4*R**, 19*R**. Diterpene aldehydes, such as **10**, tend to form complex cyclic hemiacetals during extraction with MeOH/CHCl₃; thus **1** could be an artifact formed from its corresponding hemiacetal (C₂₀ compound) during this process.

Compound **2** was obtained as an optically active, clear yellow oil and displayed absorption bands for conjugated carbonyl (1671 and 1623 cm⁻¹) and hydroxy (3483 cm⁻¹) functionalities in its IR spectrum. The molecular formula of **2**, which was deduced as C₂₀H₃₂O₂ by HRESIMS ([M + Na]⁺, *m/z* 327.2292), required five degrees of unsaturation. As analysis of the NMR data (Tables 1

Table 2. ^1H NMR Data of Compounds **1**–**4** (400 MHz in CDCl_3 , J in Hz)

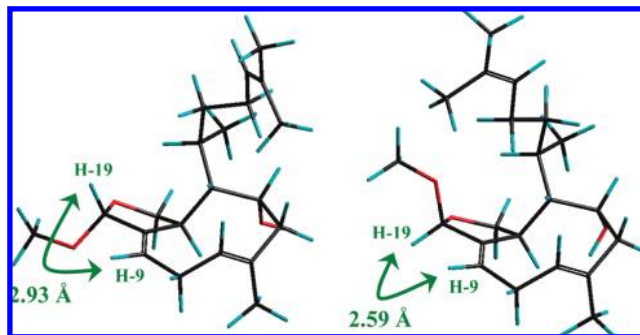
position	1	2	3	4
2	3.02, br d (6.0)		4.08, d (2.0)	1.53, m
3	1.99, m	6.36, s	2.86, d (2.0)	2.93, dd (10.0, 3.0)
4	4.26, nr ^a			
5a	2.14, dd (13.5, 4.0)	1.96, m	1.18, m	1.18, m
5b	2.31, dd (13.5, 2.0)	3.12, br d (11.0)	2.05, m	2.11, m
6a		1.80, m	2.11, m	2.10, m
6b		2.72, dd (12.5, 6.0)	2.38, m	2.33, m
7	5.34, dd (11.5, 4.0)	4.97, br d (12.5)	5.07, d (12.0)	5.08, br d (10.0)
8a	2.74, ddd (16.0, 7.5, 4.0)			
8b	3.14, ddq (16.0, 11.5, 1.5)			
9a	5.84, dddd (7.5, 1.5, 1.5, 1.5)	1.62, m	2.06, m	2.07, m
9b		2.21, td (14.5, 2.0)	2.41, m	2.32, m
10a	2.01, m	1.40, m	1.73, m	1.57, m
10b		2.03, m		1.73, m
11a	1.09, m	2.27, ddd (12.0, 8.0, 3.0)	1.97, m	1.54, m
11b	1.20, m			
12	1.92, dt (7.5, 7.5)	1.76, m	1.72, m	1.65, m
13a	5.08, thept (7.5, 1.5)	1.62, m	1.61, m	1.36, m
13b		1.95, m	1.97, m	1.55, m
14a		1.41, m	1.63, m	1.41, m
14b		2.00, m	1.90, m	1.52, m
15	1.59, br s	1.07, s	1.26, s	1.26, s
16	1.68, br s	1.81, s	1.52, s	1.27, s
17	1.09, d (7.0)	1.65, s	1.74, s	1.69, s
18a	3.81, dd (9.5, 6.0)			
18b	4.09, d (9.5)			
19	5.19, br d (1.5)	1.26, s	1.26, s	1.17, s
20	1.86, br s	1.27, s	1.12, s	1.24, s
21	3.40, s			

^a Not resolved.**Figure 1.** Key ^1H – ^1H COSY (–) and HMBC (C to H) (→) correlations for compound **1**.**Table 3.** Most Stable Conformation^a of Selected Diastereoisomers of Compound **1**

diastereoisomer	ϕ (H-2, H-3)	3J (Hz) ^b	ϕ (H-3, H-4)	3J (Hz) ^b	$d_{\text{H-3/H-7}}$ (Å)
2 <i>R</i> , 3 <i>S</i> , 4 <i>R</i> , 9 <i>E</i>	50°	4.5	–109°	2.6	1.8
2 <i>R</i> , 3 <i>S</i> , 4 <i>R</i> , 9 <i>Z</i>	–60°	3.2	76°	1.5	6.2
2 <i>R</i> , 3 <i>R</i> , 4 <i>S</i> , 9 <i>E</i>	–170°	11.4	–58°	3.6	4.3
2 <i>R</i> , 3 <i>R</i> , 4 <i>S</i> , 9 <i>Z</i>	154°	9.9	83°	0.6	5.2
2<i>S</i>, 3<i>S</i>, 4<i>R</i>, 9<i>E</i>	–95°	1.2	–87°	0.8	1.8
2 <i>S</i> , 3 <i>S</i> , 4 <i>R</i> , 9 <i>Z</i>	113°	2.7	73°	1.8	6.2
2 <i>S</i> , 3 <i>R</i> , 4 <i>S</i> , 9 <i>E</i>	101°	1.4	–67°	2.4	4.7
2 <i>S</i> , 3 <i>R</i> , 4 <i>S</i> , 9 <i>Z</i>	53°	4.3	–88°	0.8	4.8

^a Determined using HyperChem Release 8.05 Pro for Windows (Hypercube, Inc., Gainesville, FL). ^b Estimated using MestReJ v1.1.⁴⁵

and **2**) revealed the presence of a β,β -disubstituted α,β -unsaturated ketone [δ_{H} 6.36 (s, 1H); δ_{C} 208.7 (s), 154.4 (s), and 121.6 (d)] and a trisubstituted double bond [δ_{H} 4.97 (br d, 1H, $J = 12.5$ Hz); δ_{C} 124.2 (d) and 135.4 (s)], **2** must be bicyclic. A careful analysis of ^1H and ^{13}C NMR, ^1H – ^1H COSY, HSQC, and HMBC experiments demonstrated that **2** possessed a dolabellane carbon skeleton. The Me-15 signal at δ_{H} 1.07 (s) showed HMBC correlations with C-1, C-2, C-11, and C-14, which placed the ketone next to the ring junction. The Me-16 signal at δ_{H} 1.81 (s) correlated with C-3, C-4, and C-5, allowing it to be placed as part of the α,β -unsaturated ketone group. Sequential ^1H – ^1H COSY correlations between H-3/

**Figure 2.** Conformation of the two epimers at C-19 of compound **1** [**1a** (left) and **1b** (right)].

H-5b, H-5a/H-6b, and H-6a,b/H-7 required the trisubstituted double bond to be positioned at C-7. The HMBC correlations between the signal of Me-17 at δ_{H} 1.65 (s) and C-7, C-8, and C-9 allowed completion of the substitution pattern of this double bond. The presence of an 11-membered ring was finally confirmed by HMBC correlations from C-7 to H-9b, C-10 to H-9b, and C-11 to H-9a and H-10a, as well as ^1H – ^1H COSY correlations between H-9b/H-10a,b and H-10a/H-11. The second ring was defined as a cyclopentane moiety by long-range HMBC correlations from C-11 to H-12 and H-13a and from C-12 to H-13b and H-14a, together with COSY correlations between H-11/H-12, H-12/H-13a,b, and H-13a/H-14a. The connection between these two rings was confirmed by characteristic HMBC correlations from C-1 to H-10b, H-11, and H-14b. Thus a typical 2-(2-hydroxypropyl) side-chain [δ_{H} 1.26 (s, 3H) and 1.27 (s, 3H); δ_{C} 26.6 (q), 29.8 (q), and 73.9 (s)] was localized at C-12 thanks to HMBC correlations from C-12 to H₃-19 and H₃-20. The geometries of the $\Delta^{3,4}$ and $\Delta^{7,8}$ double bonds were defined to be *Z* on the basis of (i) downfield shifts of respectively C-16 and C-17 vinyl methyl carbons (δ_{C} 30.4 and 22.6, respectively) and (ii) NOE cross-peaks between respectively H-3/H₃-16 and H-7/H₃-17. The relative configuration at the chiral centers C-1, C-11, and C-12 was also deduced on the basis of NOE

correlations between H₃-15/H-14a, H-11/H-14b, H-11/H₃-19, and H-11/H₃-20. Indeed these data implied a *trans* fusion of the two rings of the dolabellane and a *trans* orientation of H-11 with respect to H-12. Compound **2** is thus (1*S**,3*Z*,7*Z*,11*S**,12*R**)-18-hydroxy-dolabella-3,7-dien-2-one.

Compound **3** was isolated as an optically active, yellow oil for which HRESIMS established the molecular formula as C₂₀H₃₄O₃ (345.2404 [M + Na]⁺), possessing four degrees of unsaturation. IR spectroscopy indicated the presence of hydroxy functionalities (3313 cm⁻¹), as did the ¹³C NMR data [δ_C 72.4 (s) and 81.7 (d)]. Two further oxygenated carbons were present in the ¹³C NMR spectrum [δ_C 63.9 (s) and 66.3 (d)], and due to their shielded nature, the presence of an epoxide function was proposed. As the occurrence of a trisubstituted double bond was deduced by ¹³C NMR signals of two sp² carbons [δ_C 125.6 (d) and 133.6 (s)], the main skeleton of **3** was defined to be bicyclic. The results of 1D (Tables 1 and 2) and 2D (Table S3, Supporting Information) NMR experiments permitted the carbon skeleton of **3** to be deduced as that of a dolabellane with two hydroxy (one tertiary and one secondary) and one epoxide function. Comparison of the NMR data for **3** with those of **2** clearly indicated that differences between these two compounds lay only in modifications in the 11-membered ring. Indeed, the secondary hydroxy function was localized at C-2 due to HMBC correlations between H-2 and C-1, C-3, C-4, C-11, C-14, and C15. Moreover, a ¹H–¹H COSY cross-peak between H-2/H-3 together with HMBC correlations from C-3 to H-2, H-5a,b, and H₃-16 and from C-4 to H-3, H-5a,b, and H₃-16 allowed the localization of the epoxide group at C-3 and C-4. Finally, as in the case of **2**, additional homonuclear and heteronuclear couplings allowed the construction of the ring and positioned the double bond between C-7 and C-8. Concerning the configuration of **3**, the *E* geometry of the Δ^7 double bond was assigned on the basis of a NOE correlation between H-7 and H-9b and the shielded nature of the vinyl methyl carbon at C-17 (δ_C 16.5). Additional NOE cross-peaks between H₃-15/H-2, H₃-15/H-3, and H-2/H-3 indicated that both H-2 and H-3 were on the same face of the compound as Me-15, while NOE correlations between H-3/H-5a and H₃-16/H-5b positioned Me-16 on the opposite face. As for **2**, cross-peaks in the NOESY spectrum between H-11/H₃-20 were in accordance with a *trans* ring junction, but overlapping of signals in the ¹H spectrum did not allow an unequivocal assignment. However, as all dolabellanes isolated from *Dictyota* species have a *trans* ring junction, on the basis of biosynthetic considerations, we propose the relative configuration of **3** to be assigned as 1*S**, 2*S**, 3*S**, 4*S**, 11*S**, 12*R**.

Compound **4** was isolated as a yellow oil, whose molecular formula, C₂₀H₃₄O₂, was revealed by HRESIMS and ¹³C NMR spectroscopy. Its IR spectrum displayed absorption for a hydroxy functionality (3444 cm⁻¹), and its NMR features (Tables 1 and 2) were analogous to those of **3** with the exception that the characteristic resonances for the secondary alcohol group were missing. So, **4** was assigned as the 2-deoxy derivative of **3**. The relative configuration of the stereocenters in **4** proved to be in accordance with those depicted in **3**, 1*R**, 3*S**, 4*S**, 11*S**, and 12*R**, respectively, according to the correlations observed in the NOESY experiment.

The antifouling activity of compounds **3**, **4**, **6–9**, and fucoxanthin together with those of a standard biocide, bis(tri-*n*-butyltin) oxide (TBTO), was evaluated by their capacity to inhibit biofilm formation by *Pseudoalteromonas* sp. D41. This capacity was determined after modeling of their sigmoid dose–response curves (Table 4). TBTO is a powerful antifoulant (EC₅₀ 10 μ M in the *Pseudoalteromonas* sp. D41 adhesion bioassay). Its toxicity against a wide range of organisms, including nontargeted ones, has led to it being banned. In the bioassays of the isolated metabolites, **4**, hydroxycrenulide (**8**), and 9-acetoxy-15-hydroxy-1,6-dollabelladiene (**9**) showed low activity (EC₅₀ > 200 μ M). Compound **3**, dictyol E (**6**), and fucoxanthin exhibited a similar moderate activity, while dictyol C

Table 4. *Pseudoalteromonas* sp. D41 Biofilm Inhibition by a Standard Biocide (TBTO) and by Compounds **3**, **4**, **6–9**, and Fucoxanthin

compound	EC ₅₀ ^a (μ M)	R ² ^b
TBTO	10	0.92
3	110	0.78
4	250	0.99
6	100	0.99
7	30	0.96
8	230	0.92
9	330	0.84
fucoxanthin	70	0.92

^a EC₅₀ expressed as the concentration corresponding to 50% of the bacterial adhesion. ^b Goodness of fit of the sigmoidal dose–response curve.

(**7**) was the most potent molecule, with an EC₅₀ of 30 μ M. This last compound, which is present in relatively high amounts in the crude extract, may be implicated in chemical defense mechanisms. It would be interesting to study the seasonal variations of the chemical composition of the extracts of this *Dictyota* sp. and to try to connect these data with the fouling sequence of the species. Geographical fluctuations could also be investigated in order to determine its specificity in term of target organisms. If the activity of dictyol C (**7**) is specific to a group of foulers, this metabolite would probably be less (or not) produced in geographical areas where these organisms are absent from the fouling community of *Dictyota* sp. Cyclic diterpenes have been investigated for their antifouling properties, but it is difficult to compare their relative activities, as several bioassays have been used (see Briand³⁸ for more information). Nevertheless, antisetlement assays with larvae of barnacles (i.e., *Balanus amphitrite*) were conducted on two families of cyclic diterpenes, reninallafoulin (from *Renilla reniformis*, Octocorallia)^{39,40} and kalihinenes (from *Acanthella cavernosa*, Porifera).^{41–43} Some of the latter showed EC₅₀'s lower than that of CuSO₄, a well-known biocide and positive control often used in antifouling assays. A dolabellane diterpene isolated from *Dictyota pfauffii* inhibited the settlement of *Perna Perna* ("mussel test"),²² and these laboratory results were consistent with field studies. Dictyol E, dictyol B acetate, pachydictyol, and dictyodial purified from *Dictyota menstrualis* and *Dictyota ciliolata* were also reported as settlement inhibitors of three marine invertebrates (including the bryozoan *Bugula neritina*).²¹ Our results showed a higher activity for dictyol C (**7**) compared to dictyol E (**6**). All these elements provide evidence that such cyclic diterpenes could be involved in the prevention of fouling in *Dictyota* spp.

Experimental Section

General Experimental Procedures. Optical rotations were measured on a Perkin-Elmer 343 polarimeter (10 cm microcell). Ultraviolet spectra were recorded in MeOH on a Shimadzu UV-2501PC spectrophotometer. IR spectra were recorded on a Jasco J-410 infrared spectrophotometer as KBr plates (films). 1D and 2D NMR spectra were obtained at 400 and 100 MHz for ¹H and ¹³C, respectively, on a Bruker Avance 400 MHz NMR spectrometer in CDCl₃. All chemical shifts were referenced to the solvent peaks (δ_H 7.26 and δ_C 77.0). High-resolution mass spectra (ESIMS) were conducted on a LTQ/FT-Orbitrap mass spectrometer (Thermo Fisher). A Varian model Prostar 210 pump with RI monitoring (Varian RI-4) was used for HPLC experiments. Fluorescence measurements for the bioassay were made using an Infinit 200 microplate fluorescence reader (TECAN, Lyon, France).

Algal Material. The marine brown alga *Dictyota* sp. was collected by hand (2 m depth) at the Brusc Lagoon (43°4'28" N, 5°47'41" E) on the Mediterranean coast in July 2007 and was identified by Dr. F. Rousseau (Muséum National d'Histoire Naturelle (MNHN), Paris, France). A voucher specimen (no. PC0124208) has been deposited in the Herbarium of MNHN.

Extraction and Purification. The shade-dried material (57 g dry wt) was extracted three times with a mixture of CHCl₃/MeOH (1:1; 3 × 250 mL) at room temperature. The concentrated extracts were

combined and partitioned in a mixture of MeOH/CHCl₃/H₂O (4:3:1) to yield, after solvent removal, 5.9 g of a dark brown lipophilic extract. This extract was subjected to CC on silica gel (Si60, 40–63 μm, Merck) with a solvent gradient from *n*-hexane to EtOAc and then from EtOAc to MeOH. The fraction eluting with EtOAc/*n*-hexane (2:3) was further purified by repeated semipreparative HPLC (Merck Purospher Star RP-18e 5 μm; 10 × 250 mm; 3 mL/min) using H₂O/MeCN (1:4) to afford **2** (1.6 mg) together with **6** (dictyol E, 62 mg) and **9** (9-acetoxy-15-hydroxy-1,6-dollabelladiene, 2.7 mg). The fraction eluting with EtOAc/*n*-hexane (1:1) was subjected to reversed-phase chromatography (H₂O/MeCN, 1:9) to yield **8** (hydroxycynulide, 25 mg) and **7** (dictyol C, 18 mg). Three new metabolites, **3** (3.2 mg), **1** (1.3 mg), and **4** (2.2 mg), were purified by reversed-phase HPLC [H₂O/MeCN (1:9)] from the fraction that eluted with EtOAc/*n*-hexane (3:2). The same fraction afforded **10** (hydroxyacetyl dictyolal, 1 mg), together with a mixture of **3** with **5** (3β-hydroxydilophol, 5 mg). A late-eluting fraction [EtOAc/*n*-hexane (7:3)] was subjected to further separation on reversed-phase HPLC (H₂O/MeCN, 1:9) to afford fucoxanthin (25 mg).

Compound 1: colorless oil; [α]_D²⁵ −170 (c 0.1, MeOH); IR (film) ν_{max} 3472, 2959, 2914, 2854, 1456, 1188, 1112, 1076, 1031, 824 cm^{−1}; ¹³C and ¹H NMR (400 MHz, CDCl₃), see Tables 1 and 2 and Supporting Information; HRESIMS *m/z* 303.2339 [M + H − MeOH]⁺ (calcd for C₂₀H₃₁O₂, 303.2324).

Compound 2: clear yellow oil; [α]_D²⁵ +4 (c 0.1, MeOH); UV (EtOH) λ_{max} 242 nm (ε 4060); IR (film) ν_{max} 3483, 2965, 2933, 1671, 1623, 1456, 1376, 1173, 1143, 1112 cm^{−1}; ¹³C and ¹H NMR (400 MHz, CDCl₃), see Tables 1 and 2 and Supporting Information; HRESIMS *m/z* 327.2292 [M + Na]⁺ (calcd for C₂₀H₃₂O₂Na, 327.2300).

Compound 3: yellow oil; [α]_D²⁵ +58 (c 0.1, MeOH); IR (film) ν_{max} 3313, 2966, 2926, 2853, 1457, 1385 cm^{−1}; ¹³C and ¹H NMR (400 MHz, CDCl₃), see Tables 1 and 2 and Supporting Information; HRESIMS *m/z* 345.2404 [M + Na]⁺ (calcd for C₂₀H₃₄O₃Na, 345.2406).

Compound 4: yellow oil; [α]_D²⁵ +45 (c 0.1, MeOH); IR (film) ν_{max} 3444, 2960, 2928, 2854, 1635, 1455, 1375, 1141, 1087, 1061 cm^{−1}; ¹³C and ¹H NMR (400 MHz, CDCl₃), see Tables 1 and 2 and Supporting Information; HRESIMS *m/z* 329.2464 [M + Na]⁺ (calcd for C₂₀H₃₄O₂Na, 329.2457).

Molecular Modeling. The initial geometry of a selected diastereoisomer of **1** was built in HyperChem Release 8.05 Pro for Windows (Hypercube, Inc., Gainesville, FL). The system was optimized in molecular mechanics (MM+) to a rms (root-mean-square) gradient of 0.01 *in vacuo* (Polak-Ribière method). Length constraints (selected interatomic distances have to be smaller than 3 Å) were implemented in order to conform with experimental NOE data (NOESY cross-peaks between H-7/H-3, H₃-17/H-4, and H₃-17/H-18b). The system was then optimized with these length constraints in molecular mechanics (MM+) to a rms gradient of 0.01 *in vacuo* (Polak-Ribière method). Length constraints were then deleted, and a molecular dynamics program was run for 1 ps, with 0.01 ps steps, relaxation time 0.1 ps, to a simulation temperature of 300 K. This was followed by MM+ geometry optimization to a rms gradient of 0.2. This protocol was repeated twice, and finally, the geometry was optimized to a rms gradient of 0.01 *in vacuo* (Polak-Ribière method) using the semiempirical AM1 program in singly excited configuration interaction [RHF (restricted Hartree–Fock), charge 0, spin multiplicity 1, lowest state]. Then, configurations at C-2, C-3, C-4, and Δ⁹ were changed successively, and each stereoisomer was modeled using the same methodology.

Bacterial Adhesion Assay (adapted from Leroy et al.⁴⁴). *Pseudoalteromonas* sp. D41 was grown on VNSS (Vaatanen Nine Salt solution) at 25 °C and sampled in the stationary phase. After centrifugation, cells were suspended in sterile artificial seawater (ASW) until an optical density of 0.6 at 600 nm was achieved. Then 200 μL of ASW was inoculated on the border-row wells of the microplate (sterile black polystyrene NUNC), and 100 μL of the bacterial suspension on other wells using an eight-channel pipet. A 100 μL sample of diluted standard biocide (TBTO) and purified molecules (compounds **3**, **4**, **6–9**, and fucoxanthin) was added in the latter wells. All the concentrations were tested in triplicate. A 100 μL portion of ASW was added in six wells to constitute the bacterial adhesion control. After 15 h, the nonadhered bacteria were removed by three successive washings (36 g/L sterile NaCl solution). The adhered bacteria were fixed for 90 min at 4 °C with sterile NaCl solution (36 g/L) containing 2% formaldehyde; then bacteria were stained by adding 200 μL of 4 μg/mL DAPI (4',6-diamidino-2-phenylindole). The excess stain was removed by three further washings (36 g/L NaCl solution). The DAPI was then solubilized

in 200 μL of a 95% ethanol solution, and fluorescence was measured (λ_{exc} = 380 nm, λ_{em} = 495 nm). EC₅₀'s were determined as concentrations corresponding to 50% of the bacterial adhesion control (bacterial adhesion in ASW in six microplate wells).

Statistical Analysis. The sigmoidal dose–response curve fitting and the determination of the EC₅₀ for each compound were achieved using GraphPad Prism software.

Acknowledgment. Funding was provided by the “Provence-Alpes-Côte d’Azur” Regional Council (Y.V., doctoral fellowship) with the scientific support of the National Park of Port-Cros (Var, France). The authors are grateful to P. Robert and A. Barcelo (scientific board of the National Park of Port-Cros) for their assistance during the design of this project. We also wish to thank J. M. Guignonis (IFR 50, Faculté de Médecine, Nice, France) for HRESIMS measurements, C. Compère (Service Interfaces et Capteurs, IFREMER Brest, France) for the supply of the *Pseudoalteromonas* sp. D41 strain, and F. Rousseau (Département Systématique et Evolution, UMR 7138, MNHN, Paris, France) for taxonomic identification of the algal material. Special thanks are owed to an anonymous reviewer for insightful advice.

Supporting Information Available: Tables S1–S4 with complete NMR data together with all 1D NMR spectra of compounds **1–4**; Tables S5 and S6 with molecular modeling data for compound **1**. This material is available free of charge via the Internet at <http://pubs.acs.org>.

References and Notes

- Qian, P. Y.; Lau, S.; Dahms, H. U.; Dobretsov, S.; Harder, T. *Mar. Biotechnol.* **2007**, *9*, 399–410.
- Costerton, J. W.; Lewandowski, Z.; Caldwell, D. E.; Korber, D. R.; Lappin-Scott, H. M. *Annu. Rev. Microbiol.* **1995**, *49*, 711–745.
- De Carvalho, C. C. R. *Recent Pat. Biotechnol.* **2007**, *1*, 49–57.
- Blunt, J. W.; Copp, B. R.; Hu, W.-P.; Munro, M. H. G.; Northcote, P. T.; Prinsep, M. R. *Nat. Prod. Rep.* **2008**, *25*, 35–94.
- Kim, J. Y.; Alamsjah, M. A.; Hamada, A.; Fujita, Y.; Ishibashi, F. *Biosci. Biotechnol. Biochem.* **2006**, *70*, 2571–2574.
- Finer, J.; Clardy, J.; Fenical, W.; Minale, L.; Riccio, R.; Battaile, J.; Kirkup, M.; Moore, R. E. *J. Org. Chem.* **1979**, *44*, 2044–2047.
- Amico, V.; Oriente, G.; Piattelli, M.; Tringali, C.; Fattorusso, E.; Magno, S.; Mayol, L. *Tetrahedron* **1980**, *36*, 1409–1414.
- Enoki, N.; Tsuzuki, K.; Omura, S.; Ishida, R.; Matsumoto, T. *Chem. Lett.* **1983**, *12*, 1627–1630.
- Ochi, M.; Asao, K.; Kotsuki, H.; Miura, I.; Shibata, K. *Bull. Chem. Soc. Jpn.* **1986**, *59*, 661–662.
- Tanaka, J.; Higa, T. *Chem. Lett.* **1984**, *13*, 231–232.
- Tringali, C.; Piattelli, M.; Nicolosi, G.; Hostettmann, K. *Planta Med.* **1986**, 404–406.
- Pereira, H. S.; Leão-Ferreira, L. R.; Moussatché, N.; Teixeira, V. L.; Cavalcanti, D. N.; Costa, L. J.; Diaz, R.; Frugulhetti, I. C. P. *Antivir. Res.* **2004**, *64*, 69–76.
- Siamopoulou, P.; Bimplakis, A.; Iliopoulou, D.; Vagias, C.; Cos, P.; Vanden Berghe, D.; Roussis, V. *Phytochemistry* **2004**, *65*, 2025–2030.
- Duran, R.; Zubia, E.; Ortega, M. J.; Salva, J. *Tetrahedron* **1997**, *53*, 8675–8688.
- Alvarado, A. B.; Gerwick, W. H. *J. Nat. Prod.* **1985**, *48*, 132–134.
- Ishitsuka, M. O.; Kusumi, T.; Kakisawa, H. *J. Org. Chem.* **1988**, *53*, 5010–5013.
- Jongaramruong, J.; Kongkam, N. *J. Asian Nat. Prod. Res.* **2007**, *9*, 743–751.
- Hardt, I. H.; Fenical, W.; Cronin, G.; Hay, M. E. *Phytochemistry* **1996**, *43*, 71–73.
- Pereira, R. C.; Cavalcanti, D. N.; Teixeira, V. L. *Mar. Ecol.: Prog. Ser.* **2000**, *205*, 95–100.
- Barbosa, J. P.; Teixeira, V. L.; Pereira, R. C. *Bot. Mar.* **2004**, *47*, 147–151.
- Schmitt, T. M.; Lindquist, N.; Hay, M. E. *Chemoecology* **1998**, *8*, 125–131.
- Barbosa, J. P.; Fleury, B. G.; da Gama, B. A. P.; Teixeira, V. L.; Pereira, R. C. *Biochem. Syst. Ecol.* **2007**, *35*, 549–553.
- Culioli, G.; Ortalo-Magné, A.; Valls, R.; Hellio, C.; Clare, A. S.; Piovetti, L. *J. Nat. Prod.* **2008**, *71*, 1121–1126.
- Culioli, G.; Ortalo-Magné, A.; Daoudi, M.; Thomas-Guyon, H.; Valls, R.; Piovetti, L. *Phytochemistry* **2004**, *65*, 2063–2069.
- Mokrini, R.; Mesaoud, M. B.; Daoudi, M.; Hellio, C.; Maréchal, J.-P.; El Hattab, M.; Ortalo-Magné, A.; Piovetti, L.; Culioli, G. *J. Nat. Prod.* **2008**, *71*, 1806–1811.
- König, G. M.; Wright, A. D.; Sticher, O. *Phytochemistry* **1991**, *30*, 3679–3682.

- (27) Danise, B.; Minale, L.; Riccio, R.; Amico, V.; Oriente, G.; Piattelli, M.; Tringali, C.; Fattorusso, E.; Magno, S.; Mayol, L. *Experientia* **1977**, *33*, 413–415.
- (28) Midland, S. L.; Wing, R. M.; Sims, J. J. *J. Org. Chem.* **1983**, *48*, 1906–1909.
- (29) Sun, H. H.; McEnroe, F. J.; Fenical, W. *J. Org. Chem.* **1983**, *48*, 1903–1906.
- (30) Ireland, C.; Faulkner, D. J. *J. Org. Chem.* **1977**, *42*, 3157–3162.
- (31) Ireland, C.; Faulkner, D. J.; Finer, J.; Clardy, J. *J. Am. Chem. Soc.* **1976**, *98*, 4664–4665.
- (32) Enoki, N.; Ishida, R.; Matsumoto, T. *Chem. Lett.* **1982**, *11*, 1749–1752.
- (33) Mori, K.; Ooi, T.; Hiraoka, M.; Oka, N.; Hamada, H.; Tamura, M.; Kusumi, T. *Mar. Drugs* **2004**, *2*, 63–72.
- (34) Ohtani, I.; Kusumi, T.; Ishitsuka, M. O.; Kakisawa, H. *Tetrahedron Lett.* **1989**, *30*, 3147–3150.
- (35) Ohtani, I.; Kusumi, T.; Kashman, Y.; Kakisawa, H. *J. Am. Chem. Soc.* **1991**, *113*, 4092–4096.
- (36) Schlenk, D.; Gerwick, W. H. *Phytochemistry* **1987**, *26*, 1081–1084.
- (37) Norte, M.; González, A. G.; Arroyo, P.; Zárraga, M.; Pérez, C.; Rodríguez, M. L.; Ruiz-Perez, C.; Dorta, L. *Tetrahedron* **1990**, *46*, 6125–6132.
- (38) Briand, J.-F. *Biofouling* **2009**, *25*, 297–311.
- (39) Keifer, P. A.; Rinehart, K. L.; Hooper, I. R. *J. Org. Chem.* **1986**, *51*, 4450.
- (40) Clare, A. S.; Rittschof, D.; Gerhart, D. J.; Hooper, G. J.; Bonaventura, J. *Mar. Biotechnol.* **1999**, *1*, 427–436.
- (41) Okino, T.; Yoshimura, E.; Hirota, H.; Fusetani, N. *Tetrahedron Lett.* **1995**, *36*, 8637–8640.
- (42) Okino, T.; Yoshimura, E.; Hirota, H.; Fusetani, N. *J. Nat. Prod.* **1996**, *59*, 1081–1083.
- (43) Hirota, H.; Tomono, Y.; Fusetani, N. *Tetrahedron* **1996**, *52*, 2359–2368.
- (44) Leroy, C.; Delbarre-Ladrat, C.; Ghillebaert, F.; Rochet, M. J.; Compère, C.; Combes, D. *Lett. Appl. Microbiol.* **2007**, *44*, 372–378.
- (45) Navarro-Vazquez, A.; Cobas, J. C.; Sardina, F. J.; Casanueva, J.; Diez, E. *J. Chem. Inf. Comput. Sci.* **2004**, *44*, 1680–1685.

NP900102F